

# The Periodic Viscous Sublayer in Turbulent Flow

RONALD L. MEEK and ALVA D. BAER

University of Utah, Salt Lake City, Utah

The model of the fluctuating viscous sublayer proposed by Einstein and Li was modified by treating some of the objections to the original formulation without greatly altering the essential simplicity of the concept. The applicability of this model to the description of the important features of turbulent flow and heat transfer in ducts and of the Toms phenomenon was evaluated by comparison of predictions of the model with experimental measurements. The mean period for growth and decay of the sublayer and the magnitudes of the wall-pressure fluctuations and wall-temperature fluctuations were compared for the flow of air and liquids. Quantitative spatial features of the periodic sublayer, that is, minimum and maximum sublayer thickness and patch size in the directions normal and parallel to the flow direction, were determined.

Experimental evidence (1, 3, 10, 15, 19 to 24, 26, 28) which has accumulated over the past 35 yr., especially in the last 5 yr., overwhelmingly rejects the concept of a laminar sublayer adjacent to the bounding surfaces of a turbulent, shear flow field (30). At present, the time dependent, viscous sublayer, or partial turbulence concept, is accepted by virtually all serious investigators of wall turbulence. The relative wealth of experimental data currently available has not, however, brought about a satisfactory theory of turbulent shear flow, and it appears unlikely that a perfectly general description of turbulence will be developed in the near future. A number of authors (2, 5, 7, 18, 27, 29) have put forward theories, having various degrees of validity, intended to elucidate the behavior of the viscous sublayer. Unfortunately, if and when predictions of these theories are compared with experimental data, they often are not consistent with all of the observations.

Characteristic features of most nonsteady models of the viscous sublayer are the assumptions, based upon observation, that, at a point on the wall, turbulent fluctuations suddenly penetrate very near the surface and that, presumably until the next penetration, viscous processes dominate the flow. A description of the penetration phenomenon and a determination of the mean period between penetrations are two of the objectives of the experimental work of Kline and co-workers (15, 24, 26) and of the theory of Black (2). Once developed, the likely complexity of such a description as that under study by Black (2) will limit its direct usefulness for calculation of the

important transport processes which occur near surfaces which bound turbulently flowing streams. However, an important practical result can be obtained when it is realized that, if the penetration process, which is really the decay process of the sublayer, is very rapid, the time-averaged transport processes at the wall can be determined solely from well-understood molecular phenomena. Under most circumstances, the mean period between turbulent penetrations is the principal parameter required for a quantitative calculation of the rates of the transport processes.

A model of the viscous sublayer having great intuitive appeal and much heuristic value was proposed some time ago by Einstein and Li (8). Somewhat the same approach was presented independently by Hanratty (12). It was the purpose of the present work to reintroduce and improve this model of the viscous sublayer; to show that, though simplified and perhaps naive, it accurately describes many features of wall turbulence; and to present new data relative to the structure of the viscous sublayer.

## THE VISCOUS SUBLAYER FLOW MODEL

For purposes of model development, the conduit surfaces which bound a turbulent flow field are pictured as being covered with patches of fluid islands of hesitation (15) in which unsteady viscous flow persists. When the maximum sublayer thickness is considerably less than the characteristic dimension of the conduit, which, for definiteness, is now taken to be a circular tube, Cartesian coordinates may be used. (Cartesian coordinates would, of course, be appropriate for a description of flow between parallel planes regardless of the sublayer thickness.) The

Ronald L. Meek is with Bell Telephone Laboratories, Murray Hill, New Jersey.

$z$  axis is taken to be in the direction of the mean flow, and the  $y$  direction is into the fluid from the wall. If the dimensions of the sublayer element in the plane of the wall are larger than its thickness, the velocity in the sublayer element may be satisfactorily represented by

$$\vec{u} = [0, 0, u_z(y, t)] \quad (1)$$

If body forces and the pressure gradient term are neglected, the equation of motion reduces to

$$\frac{\partial u_z}{\partial t} = \nu \frac{\partial^2 u_z}{\partial y^2} \quad (2)$$

for a fluid having constant density and viscosity. That neglecting the pressure gradient is consistent can be demonstrated (19) for Reynolds numbers corresponding to fully developed turbulent flow.

The velocity at the outer edge of a given patch  $u_B$  is taken to be some constant, and the growth of the sublayer element in time is treated as a semi-infinite, boundary layer type of phenomenon. The development of the patch proceeds with time until a viscous turbulent transition takes place. The element then breaks up into a turbulent hash, mixes with the core, and is replaced, essentially instantaneously, with a new patch, the development of which begins, as a first approximation, at zero thickness. Then, if the time origin is taken to be the beginning of a growth cycle, the boundary conditions become

$$t = 0, y > 0, u_z = u_B \quad (3a)$$

$$t > 0, y \rightarrow \infty, u_z = u_B \quad (3b)$$

$$t > 0, y = 0, u_z = 0 \quad (3c)$$

Equation (3c) corresponds to the requirement that there should be no slip at the wall. The well-known solution to (2) is

$$u_z = u_B \operatorname{erf} \left[ \frac{y}{2\sqrt{\nu t}} \right] \quad (4)$$

This result implies a discontinuity at the wall at  $t = 0$ , which is characteristic of such simple developments, but all time averaged values are well behaved.

Introduction of the dimensionless variables  $y^+$ ,  $u^+$ , and  $t^+$  and the friction velocity  $u_*$  alters (4) to give

$$u_z^+ = u_B^+ \operatorname{erf} \left[ \frac{y^+}{2t^+} \right] \quad (4a)$$

The growth period  $T$  of the sublayer can be related to the bounding velocity  $u_B$  by use of the fact that

$$\bar{\tau}_w = \mu \frac{\partial u_z}{\partial y} \bigg|_{y=0} \equiv \frac{\mu}{T} \int_0^T \frac{\partial u_z}{\partial y} \bigg|_{y=0} dt$$

The result is

$$T^+ = \frac{2u_B^+}{\pi^{1/2}} \quad (5)$$

Thus far, the results are exactly those of Einstein and Li (8). The boundary-layer development used does not admit a well-defined sublayer thickness, which is now taken to be that point where the velocity is 99% of the bounding velocity. Then use of tables of error functions gives the result that

$$\delta^+ = 3.64 t^+$$

and, in particular, the maximum thickness and period are related by

$$\delta^+ = 3.64 T^+ \quad (6)$$

An immediate objection to the development is that growth of the sublayer should begin not from the wall but from some average minimum thickness. Evidence, to be discussed shortly, shows this thickness to be about 1.5 in dimensionless variables. It has been shown (9) that this results in only a 2% reduction in the calculated values of  $T^+$ ; thus, the period is essentially determined only by the value of  $\delta_m^+$ .

The turbulent core is treated only as a time averaged phenomenon. Viscous effects are neglected, and a mixing length theory is assumed applicable. The well-known result for turbulent pipe flow is (25)

$$\frac{d\bar{u}_z^+}{dy^+} = \frac{1}{\kappa y^+} \quad (7)$$

where  $\kappa \equiv 0.4$  is a universal constant descriptive of the eddy transport mechanism. Integration of (7) with the boundary condition

$$y^+ = \delta_m^+, \bar{u}_z^+ = 0.99 u_B^+ \quad (8)$$

yields

$$\bar{u}_z^+ = \frac{1}{\kappa} \ln y^+ + B \quad (9)$$

where

$$B = 0.99 u_B^+ - \frac{1}{\kappa} \ln \delta_m^+ \quad (10)$$

In order to relate to Reynolds number, it is to be noted that

$$\langle \bar{u}_z^+ \rangle = \frac{2}{R^{+2}} \int_0^{R^+} \bar{u}_z^+ (R^+ - y^+) dy^+ \quad (11)$$

and

$$N_{Re} = 2 \langle \bar{u}_z^+ \rangle R^+ \quad (12)$$

The closure relation for the model should be the transition criterion for the sublayer element. Stability theory (25), in conjunction with experimental measurements of the transition point for flat plate boundary layers (11), permits at best a qualitative evaluation of the transition criterion for the unsteady viscous sublayer (19). An alternative approach is to assume the validity of some empirical relation in order to effect completion of the model. Only because a theory of this viscous turbulent transition is not available, the Prandtl formula for the friction factor, which can be written as

$$\langle \bar{u}_z^+ \rangle = 4\sqrt{2} \log (2\sqrt{2} R^+ - 0.4\sqrt{21}) \quad (13)$$

is introduced. Then, five equations, (5), (6), (11), (12), (13), contain six variables,  $u_B^+$ ,  $\delta_m^+$ ,  $T^+$ ,  $R^+$ ,  $\bar{u}_z^+$ ,  $N_{Re}$ , so that the parameters can be determined as functions of the Reynolds number. In the original Einstein-Li formulation,  $u_B$  was empirically set equal to the velocity in the turbulent profile corresponding to a distance from the wall of three times the displacement thickness. This corresponds to the assumption that  $u_B^+ = 15.7$  in the present notations. The analysis presented here shows that  $u_B^+$  varies from 19.0 at  $N_{Re} = 2,100$  to 16.0 at  $N_{Re} = 2.5 \times 10^5$  (19). The computed periods agree with the Einstein-Li prediction at high values of  $N_{Re}$  and are somewhat longer for low values of the Reynolds number.

The maximum sublayer thickness as a function of Reynolds number is given in Figure 1. The maximum sublayer thickness should correspond to the outer edge of the so-called *buffer layer* which, by definition, is that region within which both viscous and turbulent effects are important. The calculated value of the maximum sublayer thickness does agree well with the older Schlichting (25) value of 70. A later value [Deissler (6)] of 26 has gained

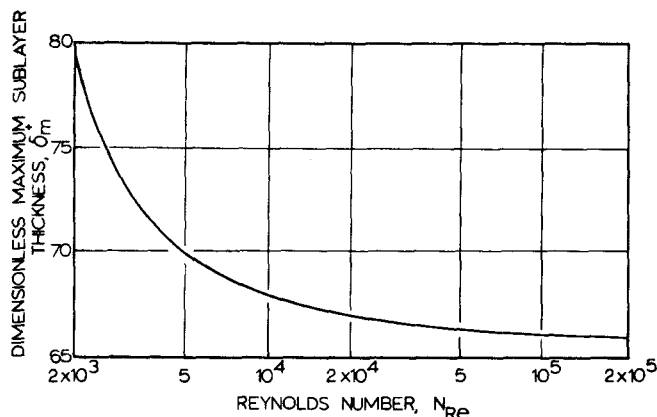


Fig. 1. Calculated maximum dimensionless sublayer growth thicknesses as a function of the Reynolds number.

some acceptance, but the recent experiments of Popovich and Hummel (22) indicate that  $\delta_m^+ \approx 35$ . The method of defining the sublayer thickness leaves much to be desired, however, and it is to be noted that it could have been defined differently, say as that point where  $\bar{u}_z/u_B = 0.90$ . Had this been done, changes in the value of  $T^+$ , which is the variable of prime interest, would be slight. So as long as consistency is maintained, and if the transport problems considered may themselves be approached from a boundary-layer point of view (that is so long as thermal and mass transfer thickness are less than the sublayer thickness), the point which is defined to be the outer edge of the sublayer is not too important.

One other point relating to the sublayer thickness and the self-consistency of the model should be noted. The condition for which the sublayer elements grow together across the duct (which must now be taken as parallel planes since Cartesian coordinates were used) is of interest since this is the lower limiting point of applicability of the model and should therefore agree with the Reynolds number for transition from laminar to turbulent duct flow. The calculated Reynolds number for this boundary-layer interaction is 2,000, which is in excellent agreement with the experimental value for the transition Reynolds number for channel flow.

Computed [by time averaging Equation (4a) over a period  $T$ ] axial velocity profiles are compared with experimental data (13, 17, 22) in Figure 2, where it is seen that agreement is excellent except near the outer edge of the sublayer where a discrepancy (in slope) exists because of the semi-infinite boundary condition. It should be noted that the constant  $B$  of Equation (10) is not a universal constant but rather varies with Reynolds number, becoming very nearly constant at very large Reynolds numbers. The unsteady sublayer behavior qualitatively explains (8, 19) the maximum in the root-mean-square fluctuating axial velocity as observed by Laufer (17), but attempts at quantitative reproduction of the experimental intensity data or of the behavior of the eddy diffusivity near the wall (14, 28) are necessarily unsatisfactory not only because of the boundary conditions but also because description of the turbulent phase of the partial turbulence is inadequate. The real virtue of the model is, however, that for description of transport phenomena, these quantities are not needed.

If the foregoing description of the sublayer is correct, and a relatively well-defined period for sublayer oscillation does exist, it would be expected that the spectra from a wall sensing device would exhibit a peak at a frequency  $f = 1/T$ . Most spectral data are presented in terms of the dimensionless variable  $fD/\langle u_z \rangle$ . The calculated value

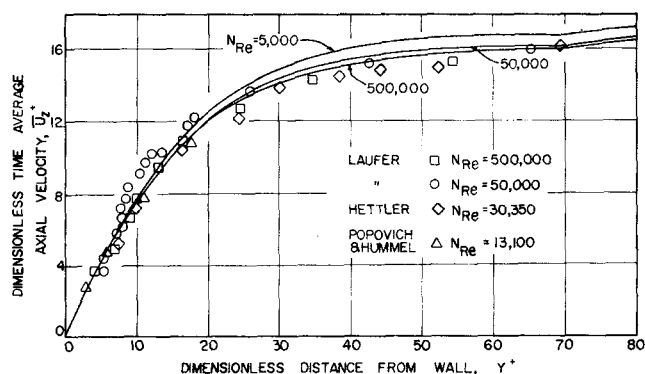


Fig. 2. Calculated time averaged velocity profiles in the sublayer compared with previously measured values.

for the period  $T$  corresponds to

$$\frac{fD}{\langle u_z \rangle} = \frac{D}{T \langle u_z \rangle} = \frac{2R^+}{T^{+2} \langle u_z^+ \rangle}$$

Consider first the pipe flow, wall pressure spectra presented by Corcos (4) for Reynolds numbers of from  $5(10)^4$  to  $2(10)^5$ . The expected spectral peak is then at  $fD/\langle u_z \rangle = 0.4$  to 1.6. The spectra presented by Corcos (4), however, show no such maxima. Rather the spectral density appears to increase by almost a factor of 10 as  $fD/\langle u_z \rangle$  decreases from 1 to 0.01. Secondly, consider the wall heat transfer fluctuation data of Armistead and Keyes (1). Their measured spectra also show no peak, but they have attempted autocorrelation and mean frequency analysis of the data. Unfortunately, the delay time for autocorrelation was not sufficient to reveal the presence or absence of the expected sublayer oscillations. The mean frequency as determined by zero crossings of the autocorrelation is, of course, not a satisfactory estimate of the characteristic frequency ( $1/T$ ), since no account of fluctuation amplitude is made. And, as their amplitude density functions reveal, the amplitude spread is rather broad, especially at low Reynolds numbers. At higher Reynolds numbers, where the amplitude density is sharper, the average frequency is at least in order of magnitude agreement with that expected on the basis of the model presented here. It is also to be noted that Armistead and Keyes' (1) measurements of the fluctuation in the heat transfer rate are in semiquantitative agreement with the predictions of the following section.

On the other hand, there are data which tend to give more direct support of this model (8, 20, 26). Mitchell's (20) mass transfer spectra indicate the existence of a peak at  $fD/\langle u_z \rangle = 0.05$  for Reynolds numbers of 1 to  $2(10)^4$  corresponding to a  $T^+$  of approximately 30 to 40. Schraub's (26) burst rate data imply (19) a value of  $T^+$  of approximately 15. The conclusion must be that presently existing data yield no definite answer as to the validity of the Einstein-Li concept.

The question then must be asked: why do present data not clearly support or refute the model? There are at least two parts to the answer. First, methods of data analysis have been such that detection of the mean sublayer period is improbable if not impossible. Second, experimentation can easily introduce signals or noise which tend to obscure the desired observation. This is especially true with regard to the low frequency vibration from valve or pump, etc. Pressure fluctuation data are particularly susceptible to misinterpretation as a result of system introduced noise. In the preliminaries to the experiments described shortly, it was noticed that low frequency fluctua-

tions were evidenced by the wall sensors even in laminar flow. These signals were eliminated only by careful adjustment of the flow system to insure a truly steady flow rate.

## HEAT TRANSFER TO A FLUID IN TURBULENT FLOW

Consideration is now given to the transmission of heat through a viscous sublayer patch from a heated wall. The fluid physical properties are taken as constant, viscous dissipation is neglected, and the size of a patch is supposed such that  $\theta = \theta(y, t)$  to a satisfactory approximation. Then the equation of energy becomes

$$\frac{\partial \theta}{\partial t} = \alpha_f \frac{\partial^2 \theta}{\partial y^2} \quad (14)$$

Fluctuations in temperature are imposed by the periodic fluctuations of the sublayer so that

$$\theta(y, t + T) = \theta(y, t) \quad (15)$$

If the fluid Prandtl number is high enough that the outer edge of the growing sublayer is always farther from the wall than the depth of significant penetration of the thermal wave, the boundary condition

$$\begin{aligned} \text{all } t, \quad y \rightarrow \infty, \quad \theta &= \theta_B \\ t = nT, \quad \delta_1 < y < \infty, \quad \theta &= \theta_n \end{aligned} \quad (16)$$

is useful, where  $\theta_B$  is a bounding temperature analogous to  $u_B$ . The maximum thickness of the thermal boundary layer is of little importance, since the wall heat flux is determined from conditions near or at the wall. Here  $\delta_1$ , the minimum sublayer thickness or that thickness not disturbed by the periodic turbulent penetration, is not necessarily taken to be zero. It is obvious that the value of this minimum thickness will be very important at high Prandtl numbers, where the penetration of the thermal wave during a growth cycle may be of the order of or less than the minimum sublayer thickness.

The one-dimensional, transient energy equation must be satisfied in the heated wall. Continuity of the heat flux and the temperature must exist at the wall-fluid interface. In order to determine the other boundary condition for the wall, explicit consideration must be given to the wall and its thermal properties. Clearly, the fluctuating sublayer imposes temperature fluctuations on the wall. If the wall is of sufficient thickness that significant fluctuation in temperature do not penetrate it, then a satisfactory boundary condition is

$$\begin{aligned} \text{all } t; \quad y \rightarrow -\infty, \quad -k_s \frac{\partial \bar{\theta}}{\partial y} &= \bar{q}_w \equiv h(\bar{\theta}_w - \langle \theta \rangle) \\ &= \text{constant} \end{aligned} \quad (17)$$

where the heat transfer coefficient  $h$  has been introduced. It will be supposed that a logarithmic, mixing length, temperature profile adequately describes the fully turbulent core (turbulent Prandtl number equals unity) when  $\langle \theta \rangle$  is evaluated.

A dimensional analysis of the differential equations for the fluid and wall and the boundary condition is straightforward and yields the result that (19)

$$N_{Nu} = N_{Nu} \left( N_{Re}, N_{Pr}, \frac{\alpha_s}{\alpha_f}, \frac{\Gamma_s}{\Gamma_f} \right) \quad (18)$$

and

$$\frac{\sqrt{\theta_w^2}}{\bar{\theta}_w - \langle \theta \rangle} = g \left( N_{Re}, N_{Pr}, \frac{\alpha_s}{\alpha_f}, \frac{\Gamma_s}{\Gamma_f} \right) \quad (19)$$

These quantities, as well as the temperature profile in the sublayer, have been determined numerically (19) for various values of the minimum sublayer thickness. The procedure was to choose an initial starting solution and to then calculate through a number of simulated sublayer oscillations until the stationary solution corresponding to periodic sublayer oscillations was converged upon. For the numerical calculation, the differential equations were put into the form of the Crank-Nicholson six point implicit representation, and the resulting tridiagonal matrix was inverted by the method of Thomas (16). Stable solutions which would have converged to known analytical solutions were obtained.

Heat transfer coefficients, based upon time average wall temperature, bulk fluid temperature, and root-mean-square wall temperature fluctuation, have been calculated for various fluids in ducts of various materials (19). The effect of change in wall properties on the calculated heat transfer coefficient was found to be very small, and a very sensitive experiment would be needed to discern such differences. A plot of calculated local Stanton number vs. Prandtl number for a Reynolds number of  $1.5(10)^4$  and various values of the minimum sublayer thickness is given as Figure 3, where a comparison to Deissler's (6) correlation of the experimental data is made. Substantial agreement is obtained if the average minimum sublayer thickness is taken to be 1.5 in dimensionless variables. Recent experimental work of Popovich and Hummel (17) gives  $\delta_1^+ = 1.6 \pm 0.4$ ; this value is the smallest value from a nonstatistical number of observations. Their observation that, for lesser distances from the wall, an essentially linear

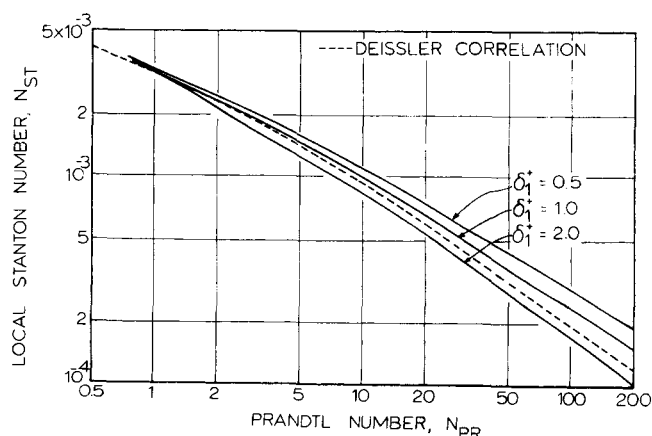


Fig. 3. Local Stanton numbers as a function of the fluid Prandtl number calculated for various assumed values of the minimum sublayer decay thickness.

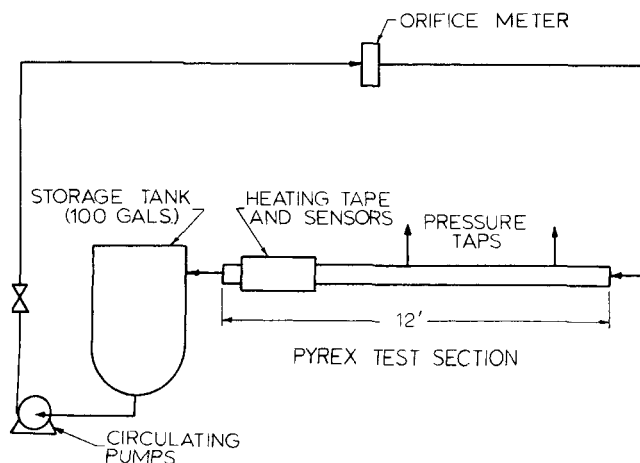


Fig. 4. Schematic diagram of liquid circulation system.

velocity gradient exists (the slope of which changes with time) can hardly be interpreted as other than additional support for consideration of the Einstein-Li type of viscous sublayer model.

As was to be expected, the root-mean-square wall temperature fluctuation was found to depend markedly on the wall properties. Experiments were performed in which the wall temperature fluctuations were measured, and, therefore, discussion of the calculated values will be delayed until the corresponding experimental data are presented.

A pronounced difference in the number of numerical computation cycles necessary to achieve convergence of the repetitious solution was noticed for high vs. low Prandtl number fluids, the latter requiring much more computation. Tests, to be described shortly, with air showed the same slow physical response in that a very much longer time was required for a constant time averaged wall temperature to be established for air than was the case for liquids.

## EXPERIMENTATION

In order to compare calculated values of the sublayer growth period to experiment, an air flow and a liquid flow system were constructed. The liquid circulation system is shown schematically in Figure 4. The air flow system employed either an ejector or small blower to circulate room air through a metering section and the test section. Measurements were made inside of 1, 2, and 4 in. I.D. steel or Pyrex tubes, and the measurement positions were 8 and 12.5 ft. from upstream disturbances for the air and liquid systems, respectively.

With air as the turbulent medium, a Thermo-Systems Model 1410 miniature pressure transducer was employed to measure wall pressure fluctuations in the test section. The sensitivity of the transducer is better than  $10^{-5}$  lb./sq. in., and frequency response is flat to 200 Hz. Because the opening into the channel was only 2 mm. in diameter, the flow disturbance introduced by the transducer was negligible. Some additional data were taken with a Thermo-Systems boundary-layer probe measuring velocity fluctuations very close to the wall ( $y^+ \approx 2$ ).

The principal sensor used in both air and liquids (tetrahydronaphthalene, Tetralin, and ethylene glycol) was a platinum film resistance element painted and fired (Hanovia Liquid Bright Platinum 05-X paint) onto the inside of Pyrex 7740 glass tubes. The film elements produced were approximately 0.0005 cm. thick by 0.01 cm. wide by 0.2 cm. long. In all but a few selected tests, the long dimension was in the direction of flow. These sensors were uncoated, which precluded the use of conductive fluids such as water in the tubes. A 1-ft. section of the tube wall was heated by means of a direct current heat-

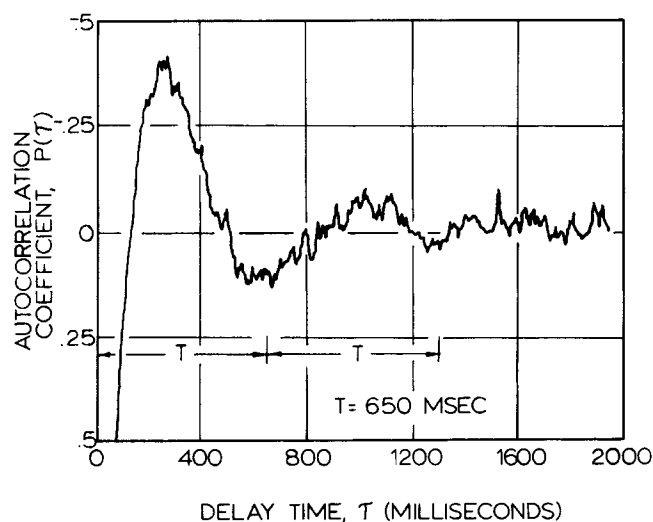


Fig. 5. Autocorrelogram from platinum film sensor for a test with Tetralin at a Reynolds number of 15,900 in a 5.26-cm. tube.

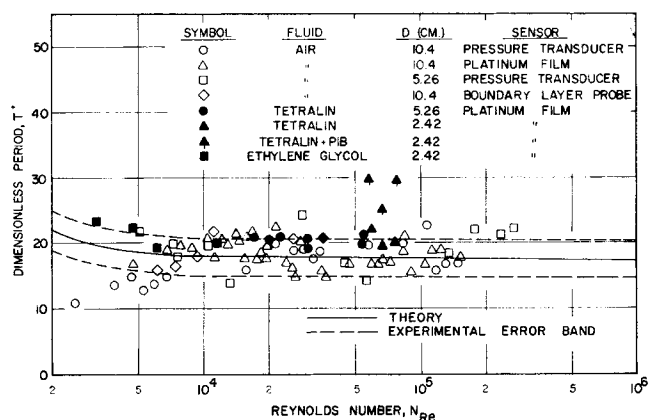


Fig. 6. Summary plot of all experimentally measured periods from autocorrelation analysis. The Tetralin-PIB solution contained 0.02% of high molecular weight polyisobutylene.

ing tape wrapped around the outside of the tube, and the film sensors were positioned in the center of this heated section. A small electrical current was passed through the platinum elements, which because of their small size and thickness were always at the local wall temperature to permit determination of wall temperature fluctuations by measurement of the voltage drop across the element. Arrays of these sensors were painted onto the tubes to permit determination of the scale of the sublayer patch at the wall.

Signals from any of the sensors were processed with Honeywell Model 104-amplifiers and stored on magnetic tape by a Precision Instrument Model 2100 tape recorder. The data were recorded at a slow speed and played back at a high speed to produce signals of a higher frequency for analysis by available instrumentation.

During the analysis of the data, it became apparent that an essentially turbulent quantity was being measured and that some distribution in growth times was observed. The model tacitly presupposes that this distribution is sharply peaked about some mean period  $T$ , and spectral analysis of the fluctuation data, by use of a Panoramic Radio Products Model LP-1a sonic analyzer, indicated a reasonably narrow distribution. The mean period  $T$  was determined from the autocorrelation coefficient, which is completely equivalent to the spectral density function, by use of a Honeywell Model 9410 Time Delay correlator. This device also permitted determination of the cross correlation coefficient between a pair of platinum film sensors and, hence, could be used when determining the sublayer patch scale. Sensor calibration and measurement of the root-mean-square value of the sensor signal yielded the fluctuation amplitude. The flow rate was measured through the pressure drop across a sharp edged orifice, and, in the case of liquids, the friction factor was also determined.

## RESULTS

A typical autocorrelation curve of the experimental data is presented as Figure 5 (wall temperature fluctuation in Tetralin). A summary of the experimental dimensionless mean sublayer periods as determined from the autocorrelation curves is presented in Figure 6, where comparison is made to the calculated values. Most of the data agree, within the experimental error, with the model prediction, and there is reasonable agreement among the data for various tube sizes, fluids, and sensors. The liquid data, however, are consistently about 20% greater than the predicted values. Comparison of data at the same Reynolds number, but at different wall temperatures, indicates that this may be caused by variation in the liquid viscosity as a result of heating the wall (19).

The raw pressure transducer data indicated several sharply peaked frequencies, and the magnitude of the fluctuation was considerably larger than that measured by

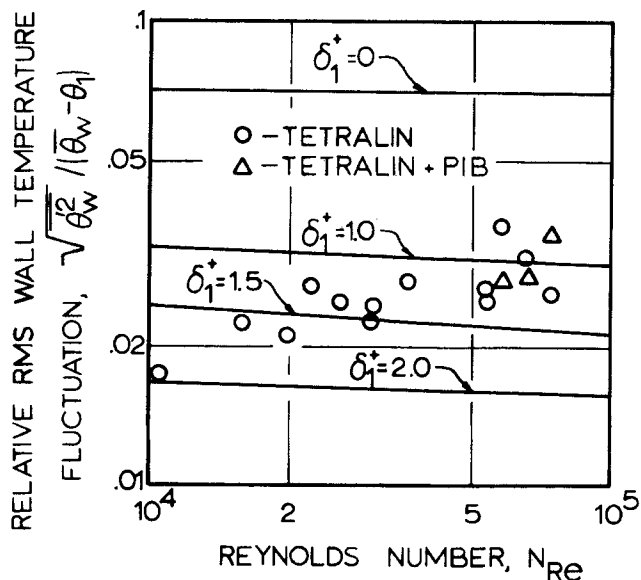


Fig. 7. Measured values of the relative root-mean-square wall temperature fluctuations for tetralin in heated Pyrex tubes. The lines for  $\delta_1^+$  are for calculations with assumed values of the minimum decay thickness.

others (4). The anomaly was immediately identified as due to the organ pipe frequencies of the air-flow system. When these frequencies were electronically removed by filtering, the resulting fluctuation magnitude was in agreement with that measured by others (4). The spectra are qualitatively the same as in previous work for  $fD/\langle u_z \rangle > 1$  but are, in fact, peaked at  $f \gtrsim 1/T$  and drop off rapidly for lower frequencies. The autocorrelation curves, from which the mean period was determined, are essentially the same in appearance as those from the platinum film data. The velocity fluctuation data did not contain the spurious signals, and the spectra did not drop off as rapidly with frequencies greater than  $1/T$  as was the case for the pressure spectra, which is in agreement with Mitchell's (20) findings.

Although the root-mean-square relative wall temperature fluctuation was measured for all platinum film, heated wall experiments, meaningful comparison with the calculations mentioned previously is possible only for the case of Tetralin as the fluid. For air, there is evidence (19) that the value of the temperature fluctuation is sensitive to the wall-to-fluid temperature difference, presumably due to the density temperature effect in air. At the low values of the Reynolds number, it was necessary to use a wall-to-air temperature difference of about  $200^\circ\text{C}$ . to obtain a satisfactory signal-to-noise ratio. The ethylene glycol used was found to contain some water, which apparently provided a variable electrical current path around the sensor and produced anomalously large apparent wall temperature fluctuations. The Tetralin data are compared with calculations in Figure 7. A value of the minimum thickness of 1.5 in. dimensionless variables gives adequate agreement with the data, lending further support to the model concept as well as experimental confirmation of the minimum thickness value inferred from comparison to heat transfer data.

Cross correlation coefficients vs. (dimensionless) sensor separation are plotted in Figures 8 and 9. The circumferential cross correlation indicates a rather well-defined structure around the circumference of the tube. The circumferential integral scale determined from the curve through the data of Figure 8 is

$$\Delta_x^+ = 18$$

Since the correlation coefficient does vary from positive to negative, it was supposed that the separation between maximum correlation and maximum anticorrelation is the extent to which the sublayer grows and decays in phase; that is, at any time, there exists a pattern of sublayer elements around the circumference of the tube which, at least for several elements, are alternately in and out of phase. If this description is correct, then the data indicate that

$$\Delta_x^+ \simeq 60$$

In the case of axial sensor separation (Figure 9), there is a much more pronounced scatter in the data, some of which may be traced to a Reynolds number dependency. The axial integral scale is

$$\Delta_z^+ = 320$$

Though computation of the extent of the sublayer patch in the axial direction is somewhat obscure, it was supposed that

$$\frac{\Delta_z^+}{\Lambda_z^+} \simeq \frac{\Delta_x^+}{\Lambda_x^+}$$

in which case

$$\Delta_z^+ \simeq 1,000$$

The data do not suggest that a well-defined structure exists along the axial direction. These values for the extent of the unit sublayer patch are in agreement with the results of other investigators (20, 24) as well as with order of magnitude estimates (19).

#### THE TOMS PHENOMENON

For some time (31), it has been observed that introduction of very small amounts (in some cases less than 0.01% by weight) of certain polymers into an otherwise Newtonian solvent will reduce the pressure drop in turbulent pipe flow by as much as a factor of 2, even though the apparent viscosity of the fluid is not appreciably changed. Perhaps the most important experimental results obtained thus far are those of Wells and Spangler (33), who have introduced the drag reducing agent at the center and at the wall of a tube containing turbulently flowing solvent. When the agent is introduced at the wall, pressure drop reduction is almost instantaneous, but when it is introduced at the center, no reduction takes place until the agent has had time to diffuse to the wall. Furthermore, Elata (9) has shown that the sublayer region is thickened

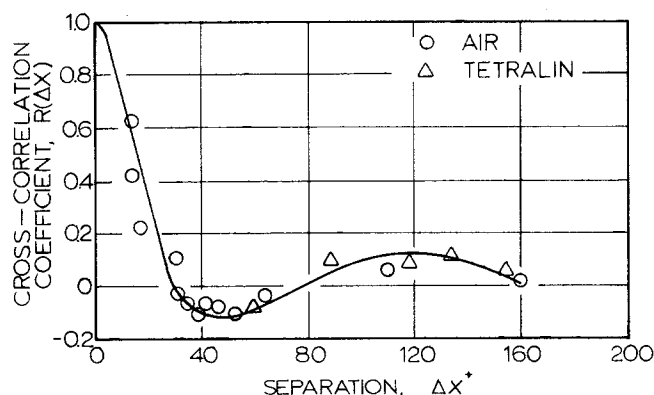


Fig. 8. Cross correlation coefficients determined by platinum film sensors separated in the circumferential direction in the 10.4- and 5.26-cm. tubes.

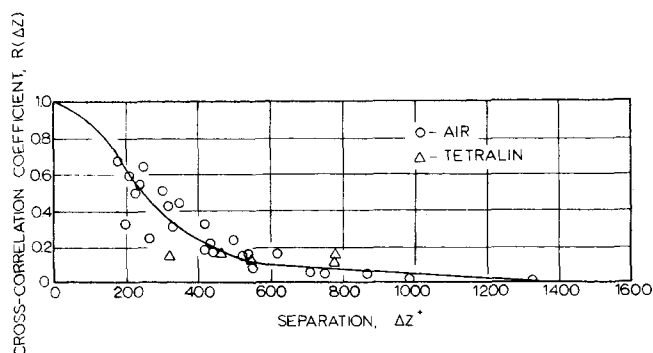


Fig. 9. Cross correlation coefficients determined by platinum film sensors separated in the axial direction in the 10.4- and 5.26-cm. tubes.

in such flows.

The periodic sublayer model was employed for calculations with a Maxwell constitutive equation replacing the Newtonian relationship (19). The principal result of the development is that when the characteristic relaxation time of the fluid is much less than the growth period, the growth period and maximum thickness are increased and friction reduction takes place. As before, the transition criterion is lacking.

Experiments were performed with an 0.02% by weight solution of polyisobutylene (Esso Vistanex L-140) in Tetralin. The mean sublayer period was measured as before, and the increase in period was found to be in agreement with that calculated, thus confirming the basic conceptual validity of the proposed sublayer model (Figure 6). The predicted dependence of the period on the friction factor was observed. The physical interpretation is that elastic effects stabilize the sublayer such that it grows to a greater thickness over a greater period of time, which results in a smaller time averaged wall shear stress. Further work is indicated in order to explain the recent important experimental findings of Virk (32), which seem to be related to the relative magnitudes of relaxation time and sublayer growth time to the onset of the friction reduction and to the effect of elasticity on stability and transition to the upper asymptotic limit of the effect of friction reduction.

## CONCLUSIONS

It can be justifiably concluded that the proposed model does indeed describe the viscous-turbulent-interaction processes occurring near a surface. Processes which depend upon time averaged phenomena, such as transport energy or mass, can be adequately predicted by use of the model in its present form. Useful application of this concept to the treatment of nonisothermal and/or non-Newtonian turbulent flow, of mass addition through the turbulent boundary layer, and of mass transfer at high rates and with chemical reaction appears to be feasible. Processes which depend upon the intimate structure of the flow field, such as those which are important in determination of eddy diffusivity and the velocity fluctuations, cannot now be evaluated. Further development of the model is indicated.

Refinement of an essentially simple model can lead only to increased complexity and loss of heuristic value. Unfortunately, the process under consideration is too complex for a simple analogue, and a more complete description requires greater intricacy. However, modern computational techniques permit manipulation of problems of great complexity and nonlinearity if such problems can be formulated in terms of known physical laws. The really great virtues

of the model proposed here, or its obvious extensions, are that the limiting transport processes occur during basically viscous flow situations and that the differential equations describing these processes are well known. It is, of course, assumed that the model truly describes the natural phenomena. Thus, regardless of necessary complexities or nonlinearities, solutions can be obtained for the important transport problems. Only an equation of state, a constitutive equation, and the thermal properties (or the diffusivities and rate constants) are required for a solution if appropriate fluid friction loss data are available. If an adequate theory of stability and transition for the viscous sublayer existed, even the latter information would not be required.

## ACKNOWLEDGMENT

The work reported herein was performed under NSF Grant GK-1357, and Ronald L. Meek was supported as a National Science Foundation graduate fellow.

## NOTATION

- $B$  = second constant from turbulent mixing length theory, Equation (19)
- $C$  = heat capacity;  $C_s$ , of heat capacity of wall material;  $C_f$ , heat capacity of the fluid
- $D$  = diameter of the tube
- $f$  = frequency of the growth and decay cycle,  $1/T$
- $h$  = local heat transfer coefficient based on bulk fluid temperature
- $k$  = thermal conductivity;  $k_s$ , thermal conductivity of the wall material;  $k_f$ , thermal conductivity of the fluid
- $n$  = integer greater than zero
- $N_{Nu}$  = local Nusselt number based on bulk fluid temperature,  $hD/k_f$
- $N_{Pr}$  = fluid Prandtl number,  $C_f \mu/k_f$
- $N_{Re}$  = Reynolds number based on bulk velocity,  $D\langle u_z \rangle/\nu$
- $N_{St}$  = local Stanton number =  $N_{Nu}/N_{Re}N_{Pr}$
- $q$  = heat flux;  $\bar{q}_w$ , time averaged heat flux at the wall
- $R$  = tube radius,  $R^+ = Ru_*/\nu$
- $t$  = time; the dimensionless time from start of the growth period  $t^+ = u_* \sqrt{t/\nu}$
- $T$  = sublayer growth period;  $T^+ = \frac{2u_B^+}{\sqrt{\pi}} = u_* \sqrt{\frac{T}{\nu}}$
- $u$  = velocity;  $\langle u \rangle$  bulk velocity;  $u_z$ , velocity component in  $z$  direction;  $u_B$ , velocity at edge of growing sublayer;  $u_* = \sqrt{\tau_w/\rho}$ ;  $u^+ = u/u_*$
- $x, y, z$  = rectangular Cartesian coordinates relative to a point on the wall in the transverse, normal and axial direction of a tube respectively;  $y^+ = yu_*/\nu$

## Greek Letters

- $\alpha$  = thermal diffusivity;  $\alpha_s = k_s/\rho_s C_s$ ;  $\alpha_f = k_f/\rho_f C_f$
- $\Gamma$  = thermal responsivity;  $\Gamma_s = \sqrt{k_s \rho_s C_s}$ ;  $\Gamma_f = \sqrt{k_f \rho_f C_f}$
- $\delta$  = thickness of growing sublayer;  $\delta^+ = \delta u_*/\nu$ ,  $\delta_m$ , the maximum thickness of sublayer growth;  $\delta_i$ , the minimum sublayer decay thickness
- $\Delta$  = unit sublayer extent at the wall;  $\Delta_x^+$ , the dimensionless distance between anticorrelation positions in the  $x$  direction
- $\theta$  = temperature;  $\theta_B$ , constant temperature at the edge of the growing thermal sublayer;  $\langle \theta \rangle$  bulk fluid temperature;  $\bar{\theta}_w$ , time average wall temperature
- $\kappa$  = first constant from turbulent mixing length theory,

- Equation (7)
- $\Lambda$  = integral scale;  $\Lambda_x^+$ , integral scale in dimensionless units in the  $x$  direction
- $\mu$  = fluid viscosity
- $\nu$  = fluid kinematic viscosity
- $\rho$  = density;  $\rho_s$ , density of wall material;  $\rho_f$ , density of the fluid
- $\tau$  = shear stress;  $\bar{\tau}_w$ , the time averaged wall shear stress

#### LITERATURE CITED

- Armistead, R. A., Jr., and J. J. Keyes, Jr., *J. Heat Transfer*, **90C**, 13 (1968).
- Black, T. J., paper presented at 6th Aerospace Sciences Meeting, AIAA No. 68-42 (Jan. 22, 1968).
- Clyde, C. G., Ph.D. thesis, Univ. Calif., Berkeley (1961).
- Corcos, G. M., *J. Fluid Mech.*, **18**, 353 (1964).
- Deissler, R. G., *Intern. J. Heat Mass Transfer*, **6**, 257 (1963).
- , in "Recent Advances in Heat and Mass Transfer," Edited J. P. Hartnett, ed., p. 253, McGraw-Hill, New York (1961).
- , *Phys. Fluids*, **8**, 391 (1965).
- Einstein, H. A., and H. Li, *Trans. Am. Soc. Civil Engrs.*, **82**, 293 (1956).
- Elata, C., J. Lehrer, and A. Kahanovitz, *Israel J. Tech.*, No. 1, 4, 87 (1966).
- Fage, A., and H. C. H. Townend, *Proc. Roy. Soc. (London)*, **A135**, 656 (1932).
- Granville, P. S. "The Calculations of Viscous Drag of Bodies of Revolution," 849, Navy Dept., The David Taylor Model Basin (1953).
- Hanratty, T. J., *AIChE J.*, **2**, 359 (1956).
- Hettler, J. P., P. Muntzer, and O. Scrivener, *Compt. Rend.*, **258**, 4201 (1964).
- Hughmark, G. A., *AIChE J.*, **14**, 352 (1968).
- Kline, S. J., and P. W. Runstadler, *J. Appl. Mech.*, **81E**, 166, (1959).
- Lapidus, Leon, "Digital Computation for Chemical Engineers," McGraw-Hill, New York (1962).
- Laufer, J., *NACA Rept. No. 32-119* (1961).
- Malkus, W. V. R., *J. Fluid Mech.*, **1**, 521 (1956).
- Meek, R. L., Ph.D. thesis, Univ. Utah, Salt Lake City (June, 1968).
- Mitchell, J. E., and T. J. Hanratty, *J. Fluid Mech.*, **26**, 199 (1966).
- Popovich, A. T., and R. L. Hummel, *Chem. Eng. Sci.*, **22**, 21 (1967).
- , *AIChE J.*, **13**, 854 (1967).
- Reiss, L. P., and T. J. Hanratty, *ibid.*, **9**, 154 (1963).
- Runstadler, P. W., S. J. Kline, and W. C. Reynolds, MD-8, Stanford Univ., Calif. (1963).
- Schlichting, Herman, "Boundary Layer Theory," McGraw-Hill, New York (1960).
- Schraub, F. A., and S. J. Kline, MD-12, Stanford Univ., Calif. (1965).
- Schubert, G., and G. M. Corcos, *J. Fluid Mech.*, **29**, 113 (1967).
- Son, J. S., and T. J. Hanratty, *AIChE J.*, **13**, 689 (1967).
- Sternberg, J., *J. Fluid Mech.*, **13**, 241 (1962).
- Taylor, G. I., *Brit. Adv. Comm. Aero. Rept. and Memo. No. 272* (1916).
- Toms, B. A., *1st Intern. Congress on Rheology*, **2**, 135, Holland (1948).
- Virk, P. S., Sc.D. thesis, Mass. Inst. Technol., Cambridge (1966).
- Wells, C. S., Jr., and J. G. Spangler, paper presented at the 4th Winter Meeting of the Society of Rheology (1966).

Manuscript received October 8, 1968; revision received March 17, 1969; paper accepted March 19, 1969.

# Simultaneous Noncatalytic Solid-Fluid Reactions

C. Y. WEN and L. Y. WEI

West Virginia University, Morgantown, West Virginia

Solid-fluid reactions often involve two or more simultaneous reactions because either the feed contains multiple fluid reactants or the fluid products are reactive with the solid. Three types of simultaneous reactions, independent, parallel, and consecutive, are examined in terms of the selectivity and the effectiveness factor based on the unreacted core shrinking model under isothermal conditions. Criteria for high selectivities are derived, and effects of diffusion and chemical reaction are discussed.

Noncatalytic, solid-fluid reactions are of considerable industrial importance and are readily found in chemical and metallurgical industries. A large number of examples of this system involving a single fluid reactant have been discussed (2, 3, 6). In many of the industrial operations, however, we often encounter situations in which more than two reactions are involved either because the feed contains multiple fluid reactants or because the products are reactive with the solid. For example, in the gasification of carbonaceous matter by steam and hydrogen, more than two simultaneous reactions are involved. It has been observed (7) that reaction of carbon with hydrogen is first order with respect to hydrogen and that with steam

is approximately zero order with respect to steam. The treatment involving simultaneous multiple reactions is much more complicated than that for a single reaction.

Actually there is a more important reason for studying such complex reactions. The interactions among the reactant, intermediate, and product species at the reacting surface of a solid particle, manifest themselves in some cases by striking changes in the magnitude of the overall reaction rate. Three commonly encountered systems for the complex reactions are independent reactions, parallel reactions, and consecutive reactions. In fact, all real systems fall either into one of the above classes, or a combination of the three. Some of the examples are:

Independent reactions: